

Analysis and Design of an Adjustable Bone Plate for Mandibular Fracture Fixation

by

Thomas Michael Cervantes

Submitted to the Department of Mechanical Engineering
in partial fulfillment of the requirements for the degree of

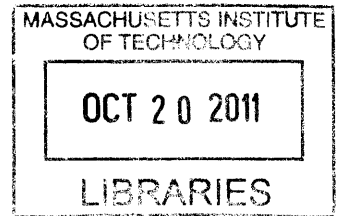
Bachelor of Science in Mechanical Engineering

at the

MASSACHUSETTS INSTITUTE OF TECHNOLOGY

June 2011

© Massachusetts Institute of Technology 2011. All rights reserved.



Author
Department of Mechanical Engineering
May 11, 2011

Certified by
Alexander H Slocum
Neil and Jane Pappalardo Professor of Mechanical Engineering
Thesis Supervisor

Accepted by
John H. Lienhard V
Samuel C. Collins Professor of Mechanical Engineering
Chairman, Undergraduate Thesis Committee

Analysis and Design of an Adjustable Bone Plate for Mandibular Fracture Fixation

by

Thomas Michael Cervantes

Submitted to the Department of Mechanical Engineering
on May 11, 2011, in partial fulfillment of the
requirements for the degree of
Bachelor of Science in Mechanical Engineering

Abstract

This thesis presents the design, analysis and testing of a bone plate for mandibular fracture fixation. Conventional bone plates are commonly used to set fractures of the mandible in a surgical setting. If proper alignment between the two bone segments is not achieved, then a malocclusion can result; this condition often causes significant discomfort to the patient, and may require costly and risky revision surgery to repair. Current methods of bone plate fixation require a surgeon to visually align the segments of bone, and once the plate has been affixed to the bone, there is little that can be done to adjust alignment of the fracture.

The modified bone plate presented here has a deformable mid-section, with the purpose of allowing a surgeon to compensate for mis-alignment observed after the plate has been affixed to the fractured bone. The mechanics of deformation associated with various adjustment mechanisms was explored analytically, numerically, and experimentally. It was found that in order to plastically deform the adjustable section, a force of 358.8 N is required, compared with a predicted value of 351 N obtained using numerical simulations and 487 N using a fixed-fixed beam model with a concentrated central load.

In addition to static tests, a dynamic testing jig has been designed with the intent of evaluating *in vitro* performance of the modified bone plate. Current ASTM and ISO standards for bone plate testing require forces to be applied to the faces of the bone plate, orthogonal to the direction of loading experienced *in vivo*. This condition is applicable to long bones such as the humerus or femur, however loading conditions of the mandible are significantly different. The testing jig allows for any bone plate of any shape to be fixed such that a force can be applied in order to simulate the normal *in vivo* loading conditions. This system could be used to further optimize the design of current and future deformable bone plates before they are incorporated into invasive animal or clinical trials.

Thesis Supervisor: Alexander H Slocum

Title: Neil and Jane Pappalardo Professor of Mechanical Engineering

Acknowledgments

First and foremost, I would like to acknowledge Alex Slocum, Jr. for guiding me through this project and helping me to find answers to all of my questions along the way.

Secondly, I would like to thank Dr. Ed Seldin for his insight into the clinical aspects of this project and patient explanations of malocclusion, maxillomandibular fixation, and general medical guidance and advice.

I would also like to thank my thesis advisor, Prof. Alex Slocum, for giving me the opportunity to complete this project; also, I grateful to him for taking a moment to explain all the cool things in the 2.007 display case to a random tour group 4 years ago- this influenced my decision to come to MIT, and it has been an honor to work on this project and others under his guidance.

Hayami Arkawa and Ken Stone at the Hobby Shop provided assistance in machining the testing jig. Pierce Hayward generously provided access to and guidance for the Instron machine used for testing. Dr. Cory Resnick graciously allowed me to shadow some of his procedures, and answered a lot of questions regarding bone plates and malocclusion.

Contents

1	Introduction	13
1.1	Mandibular Anatomy	13
1.2	Mandibular Fracture	14
1.3	Repair Techniques	16
1.4	Bone Plates	18
1.5	Malocclusion	18
2	Mandibular Bone Plate Design	21
2.1	Design Features	21
2.2	Analysis	23
2.2.1	Beam Theory	23
2.2.2	Numerical Analysis	24
2.2.3	Experimental Evaluation	26
2.2.4	Results	29
3	Testing Apparatus	33
3.1	Design Process	33
3.2	Functional Requirements	34
3.2.1	Prior Art & Literature Review	34
3.2.2	Strategy Selection	37
3.2.3	Concept Design	40
3.2.4	Risks & Countermeasures	42
3.3	Testing Protocol	44

4	Conclusions & Future Work	47
A	Beam Theory Matlab Script	49
B	Tolerance Calculations	55
B.1	Analysis for Concept 1 Shaft Misalignment	55
B.2	Analysis for Concept 2 Gap Misalignment	55

List of Figures

1-1	Relevant Anatomical Features of the Mandible	14
1-2	Fracture Occurance for Different Regions of the Mandible	15
1-3	Cross-Sectional View of the Mandible	15
1-4	Maxillomandibular Fixation (MMF) Using Arch Bars	17
1-5	Bone Plate Used in an Open Reduction Internal Fixation Procedure (ORIF) [16]	17
1-6	Typical Mandibular Bone Plate Geometry	18
1-7	Malocclusion [6]	19
2-1	Mandibular Bone Plate With Deformable Section	21
2-2	Variations Modes of Plate Deformation [22]	22
2-3	Variations Embodiments of the Bone Plate Geometry	22
2-4	Load Applied to Bone Plate by Surgeon to Manipulate Deformation .	23
2-5	SolidWorks Simulation Mesh of 56,564 4-Node Elements	25
2-6	FEA Central Loading Results	25
2-7	FEA Distributed Load Results	26
2-8	Deformable Bone Plate in the Static Testing Jig	27
2-9	Load Testing Results	27
2-10	Progression of Bone Plate Deformation (mm, in red) for Each of the Three Loading Regions	28
2-11	Attachement Used to Apply Load to Bone Plate	29
3-1	Sawbone Mandible [30]	35

3-2	Possible Loading Conditions: Cantilever (1) and Three-Point Bending (2)	36
3-3	Testing Apparatus Conforming to ASTM-F382[2] and ISO-9585[19] .	37
3-4	Design Notebook Sketch of Strategy 3	38
3-5	Testing Concept 1	40
3-6	Concept 1 Mounting Arms in Tangential Contact	41
3-7	Testing Concept 2	41
3-8	Parasitic Moments in Concept 1: Risk and Countermeasure	42
3-9	Shaft Misalignment Risk for Concept 1	43
3-10	Tolerance Risk for Concept 2	44

List of Tables

2.1	Beam Bending Equations Used to Calculate Stress and Displacement [17]	24
2.2	Material Properties for 304 Stainless Steel	29
2.3	Force Required to Achieve Yield Stress in the Bone Plate: Comparison of Results from the Analytical, Numerical, and Experimental Models	30
3.1	List of Functional Requirements	34
3.2	List of Design Strategies	38
3.3	Pugh Chart Evaluation of Design Strategies	39
3.4	List of Testing Trials	45

Chapter 1

Introduction

The goal of this work is to design an adjustable bone plate for mandibular fixation. In addition to this bone plate, a testing device is presented that enables assessment of plate performance under *in vitro* conditions. The bone plate design is currently patent pending, and this work focused on modeling and assessing *in vitro* performance of the plate. First, a literature review of mandibular fractures, repair techniques, and testing methods is presented. Then, theoretical and numerical models are developed to predict the forces needed to deform the center section of the bone plate. These findings are compared to results of an experimental evaluation. Two designs for bone plate testing apparatuses are then presented. Motivation for this research came from the need to address the problem of malocclusion by giving surgeons greater control of the occlusal relationship at the fracture site after the bone plate has been secured with screws.

1.1 Mandibular Anatomy

The mandible (lower jaw) is one of the bones that comprise the skull [21]. It exhibits bilateral symmetry across the sagittal plane. Anatomical regions of the mandible include the body, the angle, and the ramus, as illustrated in the schematic shown in Figure 1-1. Important features include the alveolar process (tooth bearing area), the condyle, the coronoid process, and the mandibular symphysis, where the two halves

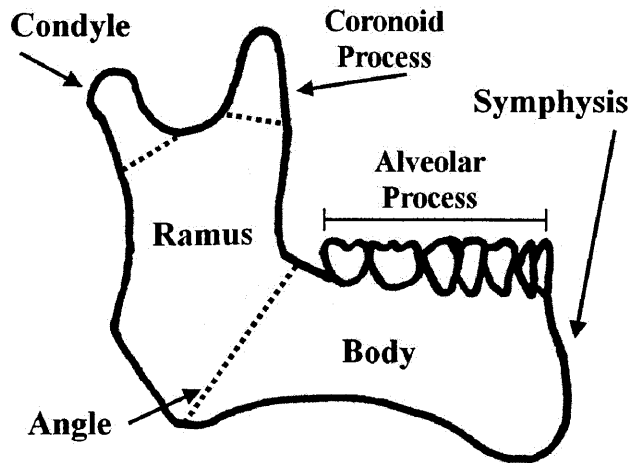


Figure 1-1: Relevant Anatomical Features of the Mandible

of the mandible join (at the chin). Adult humans normally have 16 mandibular teeth and 16 maxillary teeth.

Mastication (chewing) and speech are the principle functions of jaw activity. Actuation is provided by the masseter, temporalis, pterygoideus lateraliis, and pterygoideus medialis muscles [21]. During mastication, the mandibular teeth are brought into contact with the maxillary teeth. Each person has a unique pattern of cusps and ridges on the surfaces of their teeth that allow interlocking of the teeth when the jaw is closed. Proper alignment of the teeth, called occlusion, is important for dental well-being.

1.2 Mandibular Fracture

Fracture of the mandible is one of the most common injuries to patients who suffer facial trauma. Roughly 50% of patients admitted to the hospital with facial trauma require surgery to repair a fractured mandible [1, 10, 11, 12, 24, 29]. Almost 75% of mandibular fractures occur in males, most frequently those of age 20–30 [10, 26]. Assault is the most common cause for these injuries; other reasons include motor vehicle accidents, falls, and sports-related injuries [7, 10, 11, 14, 24, 26, 29]. Fractures can occur anywhere in the mandible, but certain patterns of injury predominate. The

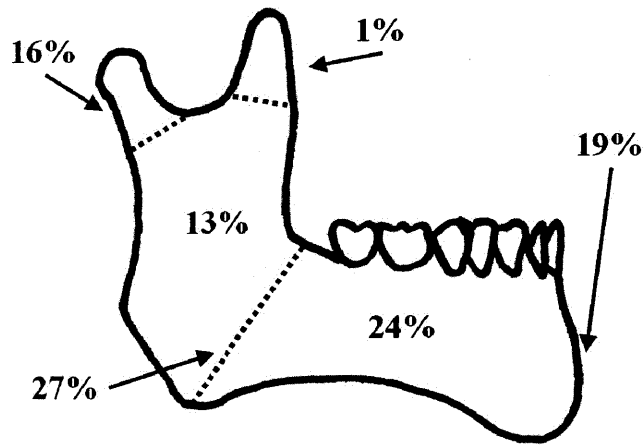


Figure 1-2: Fracture Occurance for Different Regions of the Mandible

most common sites of fracture, as shown in Figure 1-2, are at the mandibular angle and mandibular body [10, 14].

A study of the cross-sectional geometry of the mandible can help to elucidate why this bone is susceptible to fracture. During mastication, forces are applied to the superior face of the bone through teeth at the alveolar process. However, if a person is assaulted, falls, etc., forces on the jaw are usually applied along the lateral face. Figure 1-3 shows a typical cross-section view of the mandible.

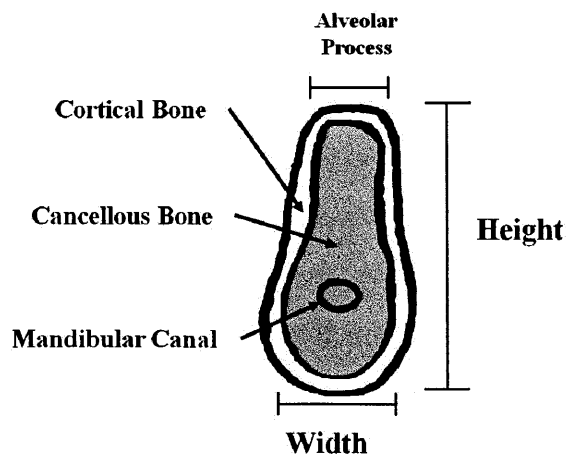


Figure 1-3: Cross-Sectional View of the Mandible

Adult males typically have a mandible height averaging between 27.6–31.0 mm, and width between 10.5–15.8 mm, resulting in an average aspect ratio of 2.3 [35]. If the cross-section of the mandible is modeled as a rectangle, then Equation 1.1 can then be used to calculate the relative area moments of inertia for each loading condition [17].

$$I = \frac{1}{12}(\textit{width}) * (\textit{height})^3 \quad (1.1)$$

If strength is defined as the maximum resultant bending stress prior to fracture in the bone, then the strength of the mandible when loaded on the lateral face is roughly 18% of that when loaded as in mastication. Thus, the mandible is very susceptible to fractures when loaded laterally.

1.3 Repair Techniques

Surgical repair of mandibular fractures is the most effective method of restoring normal anatomy. The goals of a mandibular fracture repair include: 1) the recovery of pre-injury jaw structure and 2) restoration of normal function. In order to recover the proper structure, it is necessary to restore proper occlusion; this is best achieved through a solid bony union at the fracture site [11]. Restoration of function is favored by preventing infection and by a suitable period of immobilization [11].

Two strategies are commonly used to immobilize mandibular fractures: closed reduction and open reduction [11, 13]. In a closed reduction, the fracture site is not surgically exposed; rather, the mandible is set in place against the maxillary teeth (upper jaw) [16]. This technique, called Maxillo-Mandibular Fixation (MMF), is usually accomplished by wiring the jaw shut, as shown in Figure 1-4. An advantage of MMF is that the upper jaw effectively acts as a cast for the mandible, aiding the surgeon in properly aligning the fracture halves [16]. However this technique requires the jaw to be immobilized for a number of weeks, which is uncomfortable for patients and complicates other factors such as nutritional intake, oral hygiene, and speech [11].

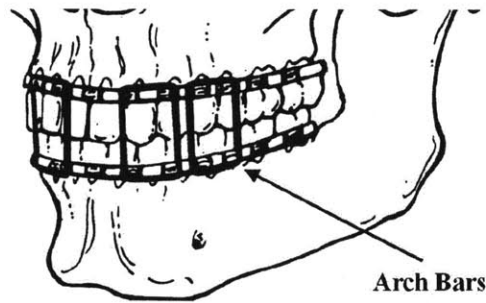


Figure 1-4: Maxillomandibular Fixation (MMF) Using Arch Bars

These days, open Reduction with Internal Fixation (ORIF) is another strategy used to achieve mandibular fixation [15]. Open reduction means that the fracture site is surgically exposed for access. Internal fixation refers to metal plates that are affixed directly to the bones by way of metal bone screws. These metal plates align the fracture site and provide fixation during the healing process. Figure 1-5 shows a bone plate after placement in an ORIF procedure. Because stability is provided by the plate, rather than fixation against the maxillary teeth, it is not necessary for the patient's jaw to be immobilized and generally does not require an external incision. Advantages of this technique include better oral hygiene during the healing process, ease of maintaining good nutritional intake, reduced risk of nerve damage, and maintaining the ability to communicate. For these reasons, ORIF with bone plates is currently the preferred method of treatment for mandibular fractures [1, 4, 5, 11, 12, 15, 36].

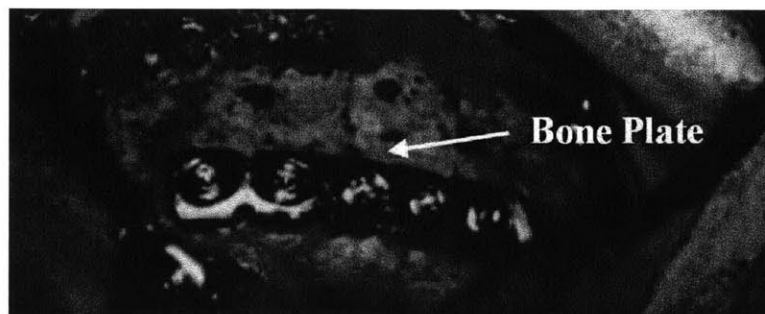


Figure 1-5: Bone Plate Used in an Open Reduction Internal Fixation Procedure (ORIF) [16]

1.4 Bone Plates

Many different types of bone plates currently exist and are used in surgery today. There are also various different techniques for applying these plates [1, 4, 5, 9, 11, 13, 15, 20, 25]. In its most basic form, a bone plate is a thin piece of metal, typically titanium, that is affixed to the bone with screws. Plates generally have a thickness on the order of millimeters; actual dimensions vary by manufacturer. Figure 1-6 shows the geometry of a typical bone plate. Depending on the repair technique used, screws can be placed through one cortical layer (monocortical fixation) or through both cortical layers (bicortical fixation). A single plate may be used or may be used in conjunction with multiple other plates in order to provide added stability.



Figure 1-6: Typical Mandibular Bone Plate Geometry

1.5 Malocclusion

Mandibular fracture repairs, while generally effective, can sometimes suffer from a number of complications. Some of the common complications that can occur with ORIF repairs of mandibular fractures can include [6, 13, 15, 29]:

- 1) Nonunion of the fracture site
- 2) Malocclusion of the fracture site
- 3) infection of the repair site
- 4) Nerve damage
- 5) Bone plate failure

Malocclusion is a significant component of patient morbidity, and can result from

improper contouring of the bone plate, improper placement or plate failure. A malocclusion occurs when there is displacement of the fracture site during healing [31]. The resulting misalignment of the teeth can cause significant discomfort and make mastication difficult for the patient. Figure 1-7 shows an intraoral picture of a severe malocclusion resulting from fracture.

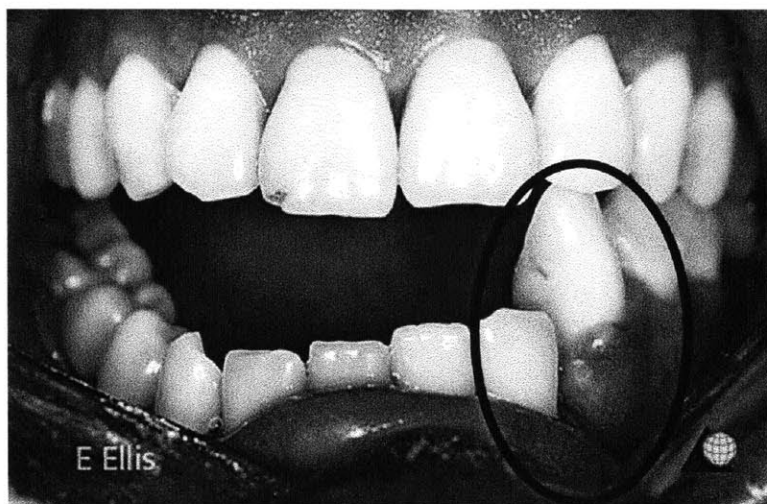


Figure 1-7: Malocclusion [6]

Malocclusion is difficult for a physician to objectively assess, but is easily noticed by the patient. A malocclusion as small as 5 microns can cause discomfort, leaving surgeons little room for error during ORIF. These small disturbances in the occlusal relationship cannot be detected by x-ray or "bite paper," but can still cause significant discomfort [28]. This places significant demands on surgeons, and the bone plates they use to treat patients, to perform as expected [33, 22].

Roughly 18% of patients who undergo treatment for a mandibular fracture suffer from malocclusion; this most often occurs in patients with associated fractures of the mandible or midfacial region [13, 31]. Malocclusion can be caused by improper placement of bone plates by the surgeon. It can also occur by loosening of the plates and/or screws after surgery [6, 5]. Treatment options for malocclusion include MMF with physical therapy, orthodontics, or further corrective surgery [5, 31].

Chapter 2

Mandibular Bone Plate Design

2.1 Design Features

The bone plate design is intended to decrease incidents of malocclusion by giving surgeons more control over alignment after the screws have been placed. This added functionality is accomplished by the addition of an octagonal deformable section to the middle of the bone plate as shown in Figure 2-1. It is expected that this plate can be used with either traditional or locking screws, monocortical or bicortical fixation, and with normal (as opposed to lagging) screw fixation [33].

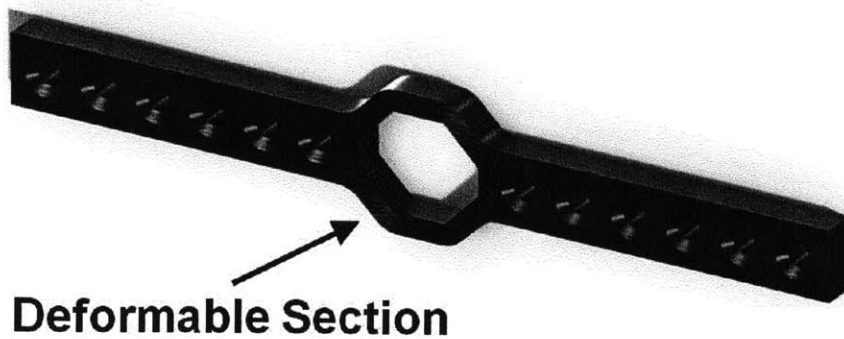


Figure 2-1: Mandibular Bone Plate With Deformable Section

The surgeon has the ability to manipulate the deformable section and adjust the alignment between the fractured ends of the mandible until malocclusion is minimized. Deformation will be effected by tool with a variable mechanical advantage, similar to

a pair of Vicegrips. This will allow a surgeon to accurately manipulate the plate by hand, discussed further in Section 2.2.1. Various modes of deformation are shown in Figure 2-2.

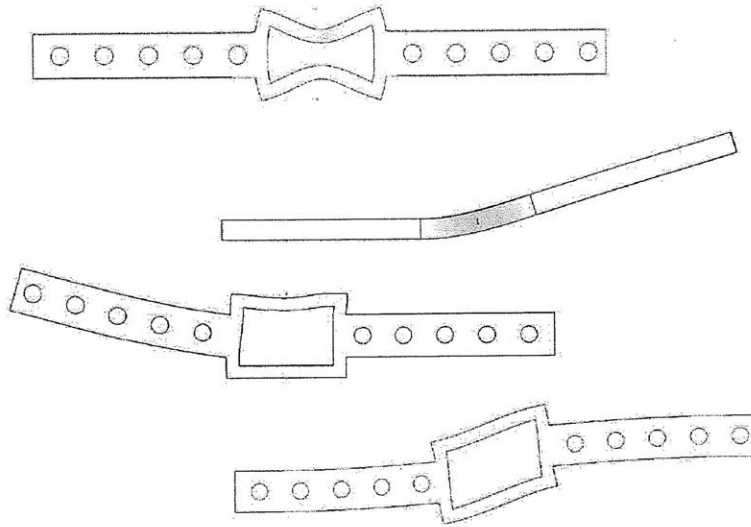


Figure 2-2: Variations Modes of Plate Deformation [22]

An octagonal geometry was initially prototyped, and a number of different geometries were considered including square, circular, and rectangular, as seen Figure 2-3 [22]. Different geometries can be used depending on the location of the fracture and the repair technique of the surgeon.

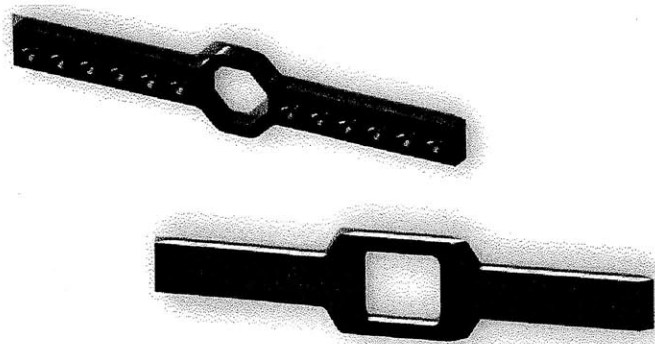


Figure 2-3: Variations Embodiments of the Bone Plate Geometry

2.2 Analysis

Functionality of this bone plate depends on the ease with which it can be manipulated by the surgeon. In order to optimize the design, models were created to find the stress and deformation resulting from applied load as a function of material and geometric parameters. Two models were used: first, a closed-form solution was found using beam theory, and then numerical model was then created. The results were then compared with an experimental evaluation. The findings of these investigations determined the best model to use for predicting behavior of the deformable section.

2.2.1 Beam Theory

During surgery the deformation of the bone plate would be caused by applied load at the deformable section. The forces required to achieve the necessary deformation dictate the type of tool needed to apply such a load. An example of this loading condition is shown in Fig. 2-4. Given this scenario, beam theory can be used to find a closed-form solution for the force needed to achieve the desired deformation.

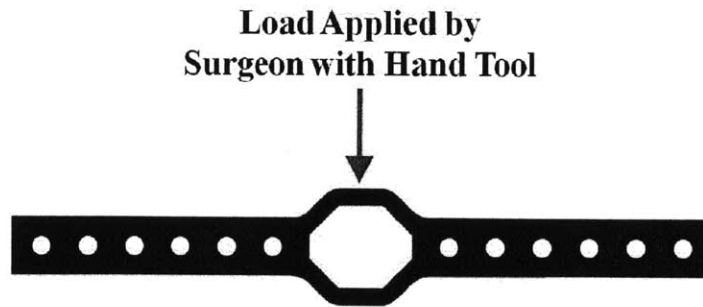
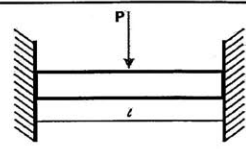
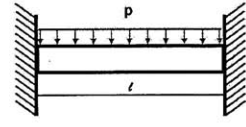
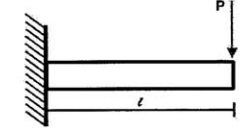
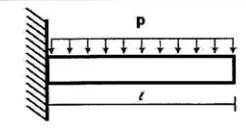


Figure 2-4: Load Applied to Bone Plate by Surgeon to Manipulate Deformation

Four different beam models were simulated for the loading condition shown in Figure 2-4. These are simple loading configurations for which exact solutions can be found using solid mechanics. Additionally, superposition applies, so results can easily be summed to find an estimate for stress and displacement. Table 2.1 shows a schematic of these loading configurations as well as the equations for maximum

stress and displacement in each beam. These equations were compiled into a Matlab [27] script to calculate the force necessary to achieve yield stress, and the resulting deformation. Appendix A contains the script that was used.

Table 2.1: Beam Bending Equations Used to Calculate Stress and Displacement [17]

Scenario	Loading Condition	Max. Stress	Max. Displacement	Schematic
1	Fixed-Fixed: Center Load	$\frac{Pl}{8}$	$\frac{Pl^3}{192EI}$	
2	Fixed-Fixed: Distributed Load	$\frac{pl^2}{24}$	$\frac{pl^4}{384EI}$	
3	Cantilever: Tip Load	Pl	$\frac{Pl^3}{3EI}$	
4	Cantilever: Distributed Load	$\frac{pl^2}{2}$	$\frac{pl^4}{8EI}$	

2.2.2 Numerical Analysis

A numerical study was conducted on the bone plate in order to determine the accuracy of the analytical model. Simulations were run using a SolidWorks Simulation[8] study. The meshing capabilities of this program allowed for the exact geometry of the bone plate to be simulated, rather than the simple beam approximation used in the closed-form model. Figure 2-5 shows the mesh of 56,564 4-node elements that was created.



Figure 2-5: SolidWorks Simulation Mesh of 56,564 4-Node Elements

Two types of loading conditions were applied: concentrated center loading and distributed loading. Figure 2-6 depicts the deformation and stresses for a concentrated load applied to the bone plate. This loading condition results in a large deformation at the site of load application, with high stress concentrations at the point of load application, and minimal stresses in other regions.

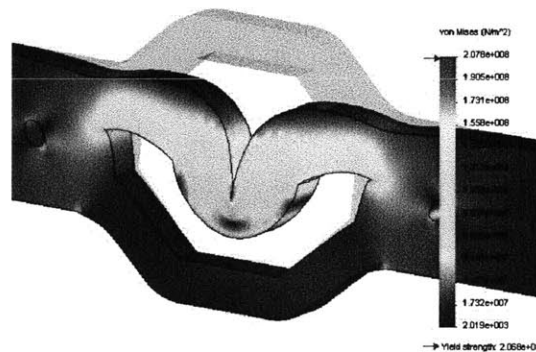


Figure 2-6: FEA Central Loading Results

A distributed loading condition was also simulated. Figure 2-7 shows the deformation and stresses for this configuration. The stresses are distributed over a much larger area than in the previous configuration, and the deformation is much smaller.

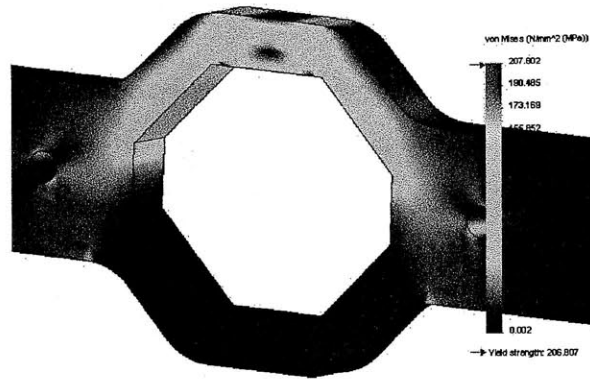


Figure 2-7: FEA Distributed Load Results

The results from the numerical analysis can be used in conjunction with the closed form analysis to predict the forces needed to deform the center section of the bone plate. Variations in the geometry of the bone plate can be taken into account so that the proper tooling can be developed for each embodiment of the plate. Numerical analysis is especially useful for predicting the deformation in irregular geometries that are difficult to model analytically.

2.2.3 Experimental Evaluation

Behavior of the plate was tested experimentally in order to compare results from the analytical and numerical modeling. A static testing jig, shown in Figure 2-8, was built to constrain vertical translation and rotation about the long axis so that testing loads could be applied to the center deformable section. The jig was milled out of aluminum stock at the MIT Hobbyshop. Most commercially available bone plates, such as those manufactured by Synthes [34], are made from titanium alloy. However, bone plates for this stage of testing were fabricated using 304 stainless steel cut with a waterjet. This was deemed an acceptable substitute because the goal of the testing was not to predict *in vivo* performance, but rather to validate the analytical and experimental models.

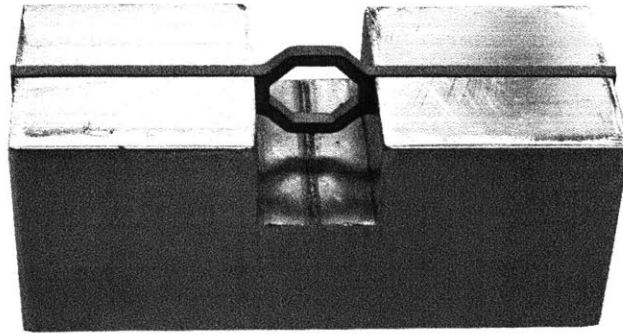


Figure 2-8: Deformable Bone Plate in the Static Testing Jig

An Instron machine [18] was programmed to apply testing loads to the bone plate at a rate of 1 mm/sec until a displacement of 5mm was achieved. A total of 4 bone plates were tested. Force and displacement data, shown in Figure 2-9, were recorded for the duration of each trial. Only one side of each bone plate was tested. However, in future testing it may be possible to use both sides of the plate. Numerical modeling can be used to determine if stresses experienced on the other side will cause plastic deformation.

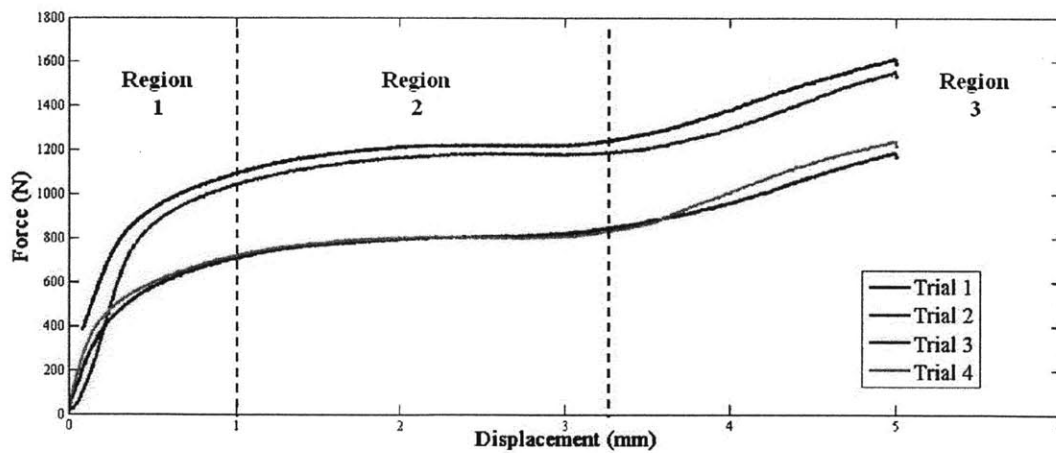


Figure 2-9: Load Testing Results

The experimental data show similar qualitative trends for each trial; three distinct regions are evident. Elastic behavior is initially seen in Region 1, followed by a transition to plastic behavior at ~ 0.4 mm. In Region 2 displacement continues with

minimal increase in load. Finally, after ~ 3.25 mm of displacement an increase in force is needed to produce further deformation in Region 3. Figure 2-10 shows the progression of deformation in each of these regions.

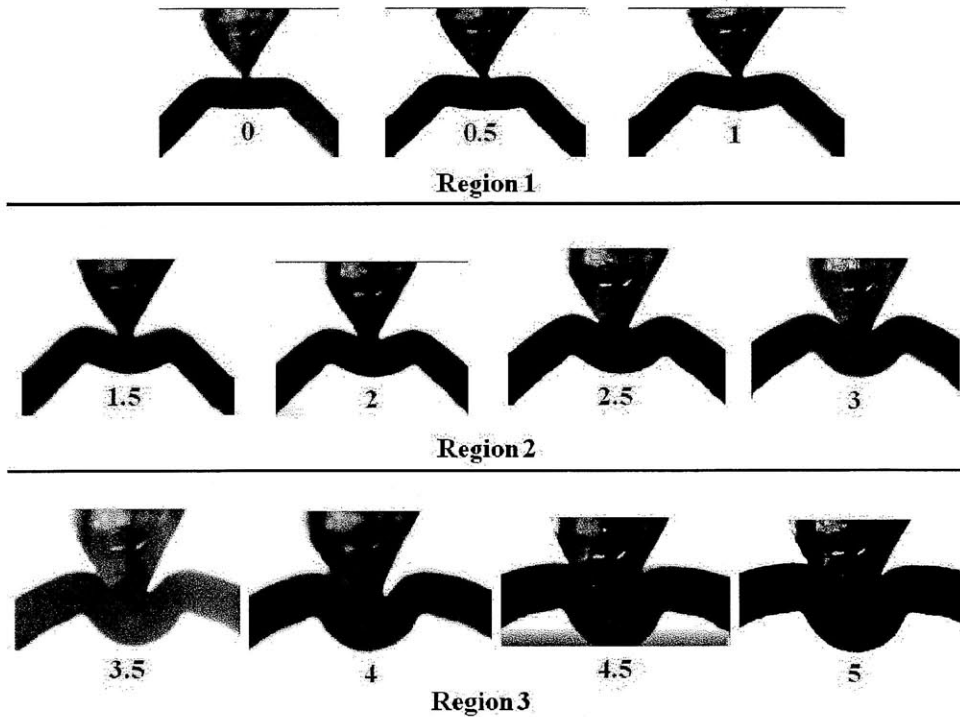


Figure 2-10: Progression of Bone Plate Deformation (mm, in red) for Each of the Three Loading Regions

The trend in Region 3 may be a result of the configuration of the experimental setup; an angled attachment, shown in Figure 2-11, was used to apply the load to the bone plate. It is possible that in Region 3 this attachment prevented the central bar of the bone plate from deforming naturally, instead causing the angled sections to bend. A different load applicator can be fabricated for future testing that would allow unconstrained deformation of the bone plate.

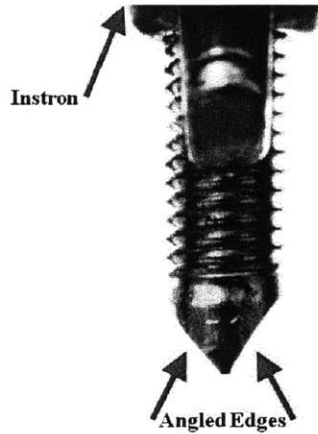


Figure 2-11: Attachement Used to Apply Load to Bone Plate

Two distinct groups are apparent in the data that were recorded. Both follow the same trends described above, but Trials 1 & 2 are offset by ~ 400 N from Trials 3 & 4. This discrepancy may have been caused by differences in the placement of the testing jig relative to the Instron machine, differences between the placement of the bone plate in the testing jig, or strain hardening in the load applicator. Future testing can incorporate a kinematic coupling such that the testing jig is always placed on the Instron stage in the same position. Regardless, more bone plates need to be tested in order to produce statistically significant data.

2.2.4 Results

Deformation of the center section of the bone plate was modeled using beam theory and numerical simulations. These models were then compared to results from experimental evaluation. The material properties of 304 stainless steel, shown in Table 2.2.4, were used in the analytical and numerical models.

Table 2.2: Material Properties for 304 Stainless Steel

	Value	Units
Modulus of Elasticity	109	GPa
Poisson's Ratio	29	N/A
Yield Strength	206.807	MPa

The analytical and numerical simulations were programmed to determine the force and resulting displacement necessary to produce yielding in the bone plate. Values from the experimental evaluation were determined from the Force-Displacement plot in Figure 2-9. A comparison of the results from the analytical, numerical, and experimental methods are shown in Table 2.2.4.

Table 2.3: Force Required to Achieve Yield Stress in the Bone Plate: Comparison of Results from the Analytical, Numerical, and Experimental Models

Model	Loading Condition	Force (N)	Displacement (mm)
Cantilever	Concentrated	122	0.0282
Numerical	Concentrated	345	0.0082
Numerical	Distributed	351	0.0082
Experimental, Trials 3-4	N/A	358.8	0.1349
Fixed-Fixed	Concentrated	487	0.0252
Experimental, Trials 1-2	N/A	791.6	0.3023
Cantilever	Distributed	973	0.0429
Fixed-Fixed	Distributed	1459	0.656

Both numerical simulations predict similar forces and deformations. However, the deformation of the simulation using a concentrated loading condition, shown previously in Figure 2-6, is a closer match to the deformation seen in experimental evaluation. Thus, it can be shown that a concentrated loading condition is the best option for future numerical studies.

The analytical model using a fixed-fixed beam with a concentrated loading condition was the closest match to the experimental results. This model matched the force data from experimental trials 3 & 4 with 26% percent error and the results from trials 1 & 2 with 38% error. Differences between the analytical model and experimental model can be attributed to geometry approximations and compressive deformations which were not accounted for. Future versions of the analytical model could incorporate these assumptions.

Displacement calculations of the analytical models differed from the experimental results by an order of magnitude; numerical calculations differed by 2 orders of

magnitude. These differences could be the result of isotropic and small-deformation approximations used in the numerical solver and inherent in the Euler-Bernoulli beam bending equations. Large deformation assumptions could be used for future versions of these models.

Experimental results show that a force between 350 and 800 N is needed to deform the bone plate. If the average human hand strength is taken to be close to 177.9 N (40 lbs), then the tool to be used to deform the bone plate must be capable of a mechanical advantage between 2 and 4.5 at its end effector. The analytical and numerical models discussed previously can be developed further to accurately calculate the forces needed to deform different embodiments of the bone plate.

Chapter 3

Testing Apparatus

The bone plate described in Chapter 2 is designed to achieve internal fixation for mandibular fracture repairs while giving surgeons control over the occlusal relationship between fracture halves. In order for this new technology to be adopted by oral & maxillofacial surgeons, the strength of this plate must equal or exceed existing plates, and it must possess the functionality to easily and sufficiently control the occlusal relationship. Thus, there are two parameters which must be tested in order to assess the performance of the bone plate: 1) strength and 2) usability.

This work focuses on the design of a testing dynamic apparatus to evaluate the strength of the bone plate relative to other plates. The motivation for choosing this approach was to prove the new bone plate design as a viable option to existing plates. Future work will focus on evaluating the usability aspects of the plate.

3.1 Design Process

A deterministic design process was followed during the design process for the testing apparatus. This included 1) development of functional requirements, 2) a prior art & literature review, 3) strategy brainstorming & selection, 4) concept development, and 5) analysis of the potential risks and countermeasures.

3.2 Functional Requirements

The functional requirements for the dynamic testing apparatus design were developed with in input from Dr. Ed Seldin [33] and Alex Slocum, Jr. [22]. Table 3.2 lists these Functional Requirements, which were drawn from the existing body of knowledge to address the scope and needs of the this apparatus.

Table 3.1: List of Functional Requirements

-
- 1) Quantify the performance of bone plates in a mandibular configuration
 - 2) Repeatable & consistent testing conditions
 - 3) Adaptable to different plate models
 - 4) Bone plate behavior decoupled from that of the testing mechanism

3.2.1 Prior Art & Literature Review

A number of studies in the literature investigate the behavior of different mandibular bone plates. A review of these studies reveals different goals and strategies that have been used to perform bone plate testing.

Two important factors that define a strategy for bone plate functionality testing are 1) the mounting substrate and 2) the loading condition. This section focuses on the ways that different studies from the literature have incorporated these factors into their testing strategy.

Mounting Condition

The mounting condition of the testing apparatus is how the bone plate is fixated. In a surgical setting, the bone plate is fixed to mandible itself using screws. Previous studies have used a number of different strategies for mounting the bone plate during testing, including:

- 1) Human mandible [7]
- 2) Sheep mandible [1, 24]
- 3) Bovine rib [3]
- 4) Synthetic mandible [11, 23]

There are clear advantages to using real bones: the bone plate can be affixed using the same techniques as in surgery. The mechanical properties of the bone are conserved, resulting in testing data that reflects the performance of the plates *in vivo*. Consistent & repeatable testing is difficult when using real bone. Many bone plates are manufactured with a standard geometry, with the intention that they are reshaped during surgery to fit the specific contours of the repair site. A bone plate of interest would need to be adjusted in this manner in order to accommodate the contours of the bone. This procedure would have to be performed by a skilled surgeon who is well-practiced in the field of mandibular repairs.

Other studies have used synthetic mandibles [11, 23]. Some, such as Sawbone mandibles (Figure 3-1), mimic the geometry and mechanical properties of bone [30]. They are available with condylar features that facilitate consistent and precise fixation using known anatomical landmarks. The properties of cortical and cancellous bone are approximated by using different composites in the cross-section of the model.

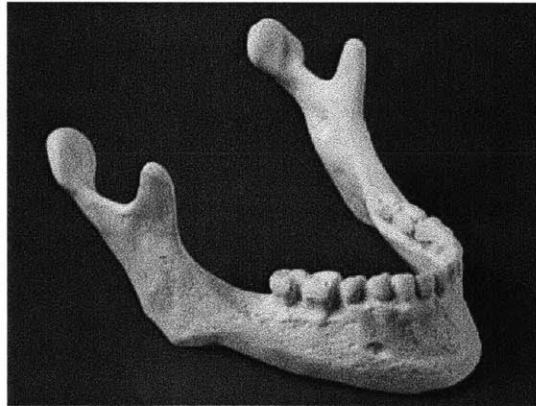


Figure 3-1: Sawbone Mandible [30]

Synthetic mandibles have certain advantages: the cost of each mandible can be significantly reduced; Sawbone mandibles range from \$20–\$70 [30]. Also their geometry

try is consistent, providing a standard configuration for each test of the bone plate. Handling of synthetic mandibles is much less logistically intense, as they do not require cleaning or freezing.

Loading Condition

The literature has shown that the human masseter muscles are capable of forces from 300N–400N for the average healthy male [9]. However, other studies have shown that patients have a post-operative bite force between 60N and 200N, with an average of 150N [20]. This is most often due to the trauma associated with surgery and muscle soreness due to hyperextension of the mandibular joint for some patients. Based on these data an optimal testing load is between 50N and 400N.

Many studies in the literature use a cantilever loading condition, with the force applied at the incisors [9, 26, 11], the anterior molar region [20] or in a unilateral molar clench [26, 25]. Others use a three-point bending configuration with the center load at the fracture site [1]. These two loading conditions are shown in Figure 3-2.

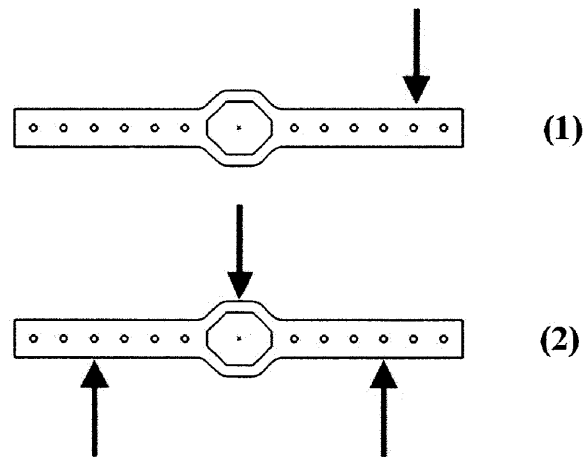


Figure 3-2: Possible Loading Conditions: Cantilever (1) and Three-Point Bending (2)

Some studies have tested in uniaxial tension [32], but this loading condition is not relevant for the present research because it is not representative of the forces experienced *in vivo*. Based on previous studies it would be optimal to have a testing apparatus that could simulate loads at each of these sites. Of these options,

three-point loading at the fracture site is most preferred because it is independent of mandible geometry.

Standards

Standards for bone plate testing have been published by ASTM international and the International Organization for Standardization (ISO). ASTM standard F382 [2] and ISO standard 9585 [19] describe a testing strategy that uses dual rolling supports to mount the bone plate, and a four-point loading condition. A significant advantage of this strategy is that the behavior of the plate is isolated from the mounting supports. Consistent & repeatable testing for a variety of bone plates can be easily achieved. Schematics of these standards are displayed in Figure 3-3.

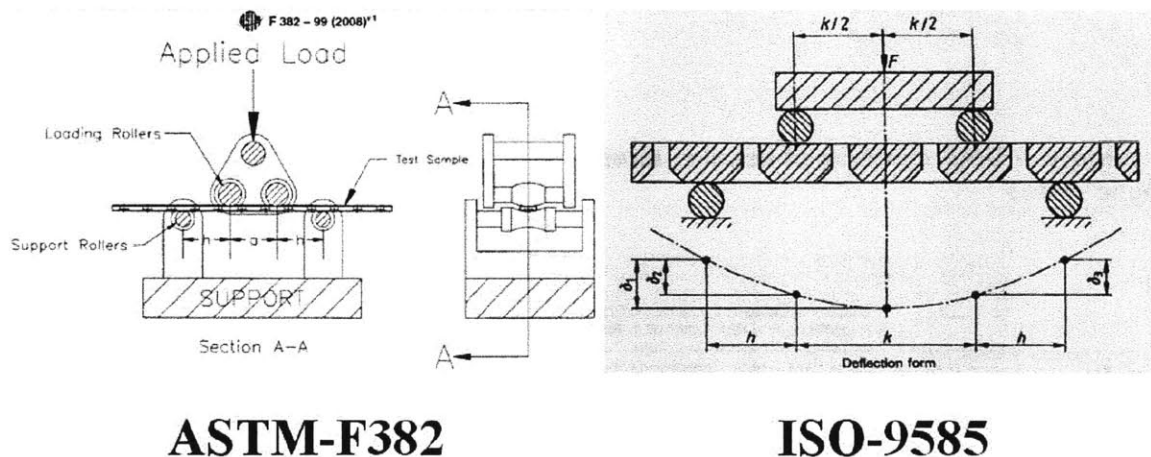


Figure 3-3: Testing Apparatus Conforming to ASTM-F382[2] and ISO-9585[19]

3.2.2 Strategy Selection

After reviewing the prior art & literature, several strategies, listed in Table 3.2.2, were developed to address the functional requirements.

Real bone is a good choice for predicting the performance of bone plates *in vivo*, but is not suited for this research because it does not allow for repeatable comparisons

Table 3.2: List of Design Strategies

- 1) Real bone
- 2) Synthetic bone, mandibular shape
- 3) Synthetic bone, other shape
- 4) Simply supported, three-point loading on lateral face
- 5) Simply supported, three-point loading on superior face

between bone plate designs. Repeatedly reshaping the bone plate in as described in Section 3.2.1 drastically reduce the repeatability of results obtained using the testing apparatus. The plate behavior would not be isolated from the behavior of the bone because they are rigidly attached.

Synthetic bone in the shape of a mandible would still require custom reshaping of the bone plates, reducing the repeatability of testing results. Furthermore, the results would be less applicable to *in vivo* performance than using real bone, and behavior of the plate is not isolated from the substrate.

A synthetic bone substrate can be made into a variety of configurations. Figure 3-4 shows a sketch of a strategy in which the bone plate is mounted to simple beams. When loaded, the beams move such that the behavior of the plate is isolated from that of the beams. This configuration allows for repeatable testing, but may be difficult to use with deformed plate geometries.

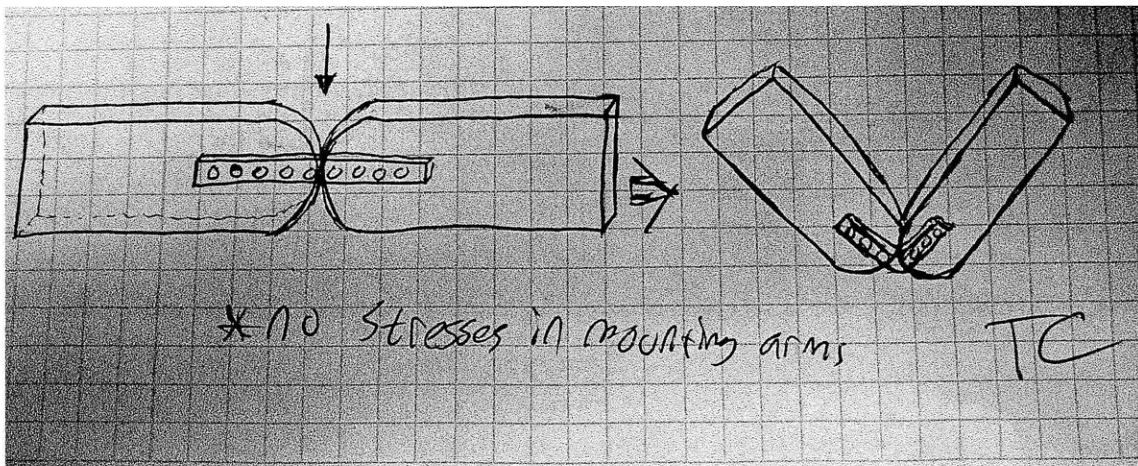


Figure 3-4: Design Notebook Sketch of Strategy 3

The simply supported mounting technique described in the ASTM and ISO standards provides a setup that is easily repeatable for a variety of plate geometries. The plate is not affixed to the apparatus, meaning that the plate behavior is isolated from that of the apparatus. However, the load is applied normal to the lateral face of the bone plate. This is not analogous to the forces experienced by bone plates *in vivo*. This strategy is sufficient to compare different bone plates against each other. However, the results would not lead to significant insight regarding the use of the bone plate in a practical setting.

An *in vitro* testing setup could be created if a load is applied to the top surface of a simply supported plate, rather than the side. This configuration would allow for repeatable testing results, and also give insight into *in vivo* performance. A possible disadvantage, however, is that testing plates with deformed geometry may be difficult.

These strategies were compared using the Pugh chart shown below in Table 3.2.2. The ability of each strategy to accomplish the Functional Requirements was weighted, and compared with a datum.

Table 3.3: Pugh Chart Evaluation of Design Strategies

Functional Requirements	Design Strategies				
	1	2	3	4	5
Quantify Performance	0	0	-1	-2	-1
Repeatable	0	+1	+3	+2	+2
Different Geometry	0	0	+1	+2	+2
Isolate Plate Performance	0	0	+1	+1	+1
TOTAL	0	+1	+4	+3	+4

The two highest scored strategies were 3 and 5: synthetic bone configured to isolate plate behavior from the testing apparatus, and three-point loading on the superior surface of the bone plate. The next step in the design process was to develop concepts to implement these strategies.

3.2.3 Concept Design

Two testing concepts were developed based off of the results from the Pugh Chart evaluation in Table 3.2.2. Concept 1, shown in Figure 3-5, uses a synthetic mounting substrate to affix the bone plate in a mandibular configuration. The bone plate is mounted on two plates with rounded ends that are initially in tangential contact. These mounting plates are then affixed to grounded columns using single fixed-pin joints. The testing load is applied with a roller at the center of the configuration, resulting in three-point bending at the fracture site. An Instron machine [18] can be used to apply the necessary loads and record data.

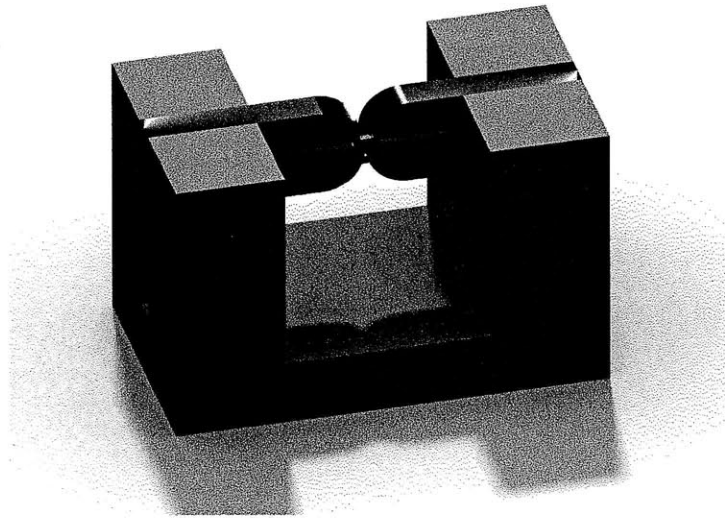


Figure 3-5: Testing Concept 1

The simplicity of this design allows for consistent & repeatable testing conditions that can be applied to a variety of bone plate geometries. The configuration of the mounting arms decouples the performance of the plate from that of the testing apparatus. As displacement increases, the rounded edges of the mounting plates roll against each other, pivoting about their mounting axes. The attachment at the mounting columns allows for unrestricted horizontal translation, as shown in Figure 3-6. This eliminates any bending, and thus concentrates all of the moment on the bone plate.

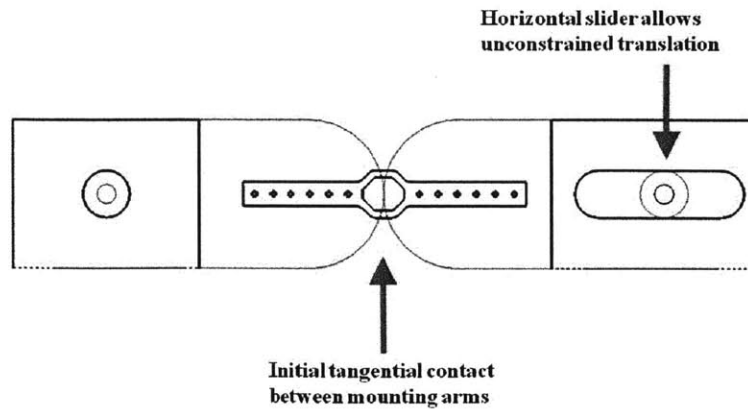


Figure 3-6: Concept 1 Mounting Arms in Tangential Contact

Concept 2, shown in Figure 3-7, applies a three-point bending load to the plate in a mandibular configuration. The bone plate is placed in the central channel and rests on two pins. A testing load is then applied to the center section. The channel keeps the bone plate in the proper orientation as it is being deformed. This concept is similar to the ASTM and ISO standards mentioned previously; however, the crucial difference is in the orientation of the bone plate during testing.

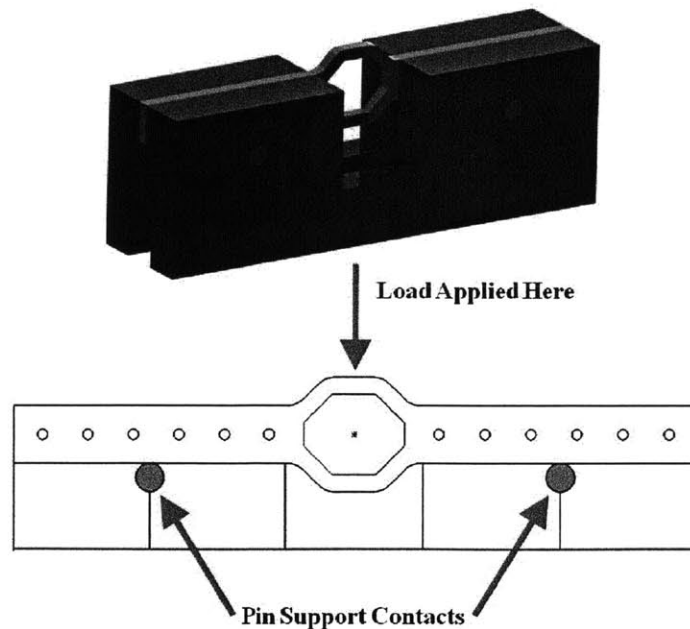


Figure 3-7: Testing Concept 2

3.2.4 Risks & Countermeasures

Potential risks were assessed for Concepts 1 & 2, and countermeasures were then identified to mitigate their effect on performance. The most critical module of both concepts is their ability to isolate the behavior of the plate from that of the testing. A risk for this MCM is that misalignment could create parasitic forces between the plate and the testing apparatus, preventing collection of data that is accurate and precise.

The testing load in Concept 1 is applied at the centerline of the bone plate. A parasitic moment is created if the centerline of the bone plate is not in line with the centerline of rotation of the mounting arm. A possible countermeasure is to affix the bone plate such that these centerlines are in line with the testing load. Figure 3-8 illustrates this risk and countermeasure.

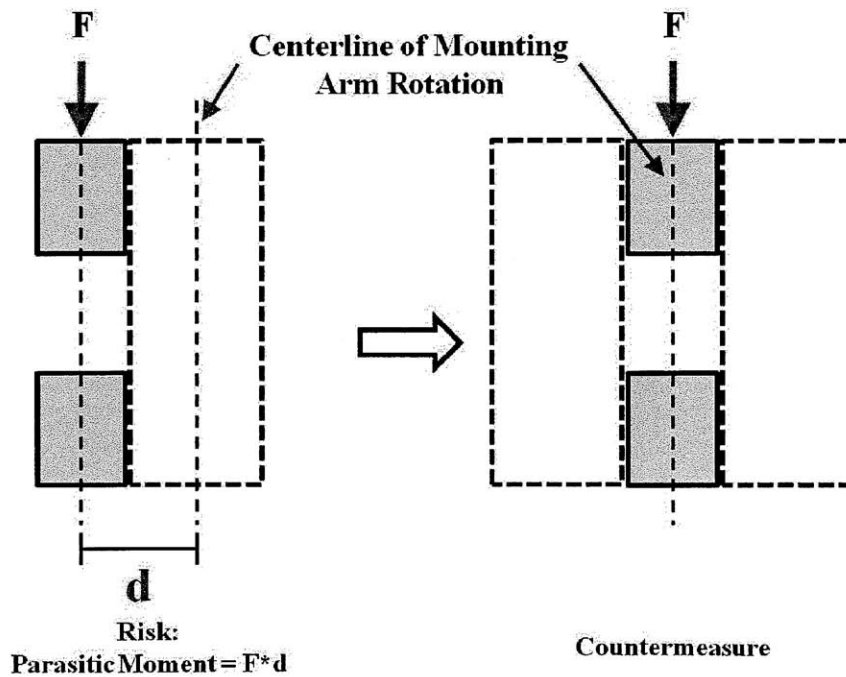


Figure 3-8: Parasitic Moments in Concept 1: Risk and Countermeasure

Shaft misalignment could also cause parasitic moments in Concept 1. The shaft of the mounting arm is set within a bearing. The arm will tilt undesireably if the gap between the shaft and the bearing is too great, as shown in Figure 3-9. The centerline of the bone plate will then be offset from the point of load application, resulting in a parasitic moment. Analysis of this error motion shows that this gap must be less than 0.0197" in order to have an offset that is less than 1% of the bone plate height. A greater tolerance can be allowed if the length of the shaft in the bearing is increased. Calculations are shown in Appendix B.1.

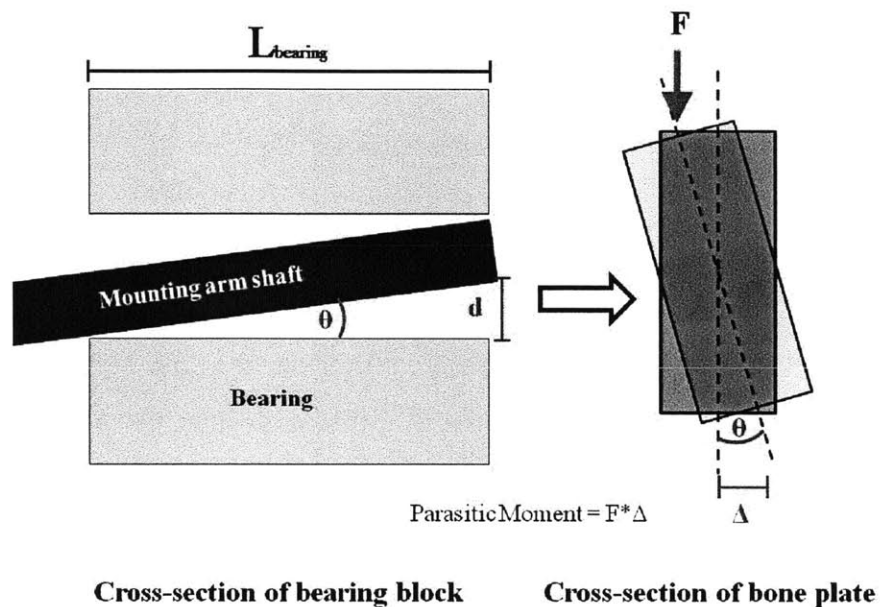


Figure 3-9: Shaft Misalignment Risk for Concept 1

Parasitic forces in Concept 2 could be generated if the central channel is too large, causing a tilt in the bone plate orientation as shown in Figure 3-10. Analysis of this error motion shows that the central channel must be machined to a tolerance of 0.0025" to have a parasitic force that is less than 1% of the applied load. Calculations are shown in Appendix B.2. This tolerance can be achieved by milling the channel out of a solid block of aluminum, as opposed to assembling the apparatus from separate parts. A 1/16" endmill must be used for this process; this requires a feed rate of 0.25 in/min at depth increments of 0.020" to ensure that the endmill does not break.

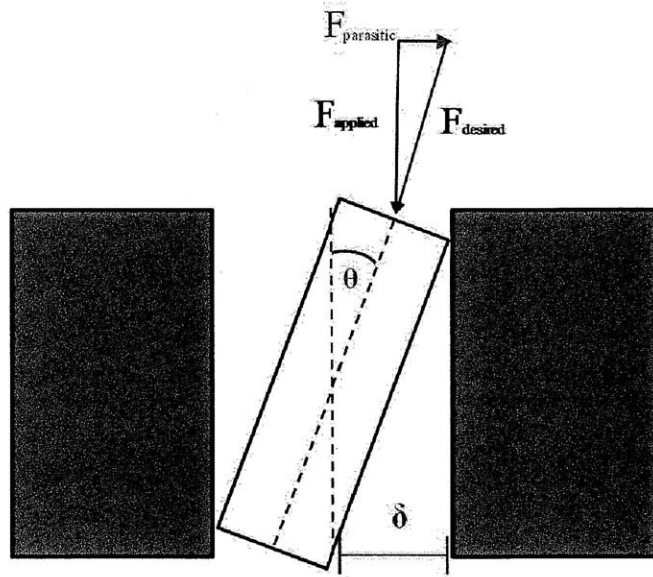


Figure 3-10: Tolerance Risk for Concept 2

3.3 Testing Protocol

Performance of the bone plate will be evaluated using the dynamic testing apparatuses described previously. Testing bone plates of differing geometries while keeping the material properties constant will give insight into the performance of the new bone plate relative to those currently used by surgeons.

Bending stiffness and force to failure will be the metrics used to evaluate relative performance of the bone plates. Bending stiffness is a standard of measurement specified in ASTM-F382, and is calculated by finding the slope of the linear elastic region of the force-displacement curve [2]. Plates with different geometries will have different bending stiffnesses; therefore this parameter can be used to compare performance between different bone plate embodiments. Force to failure will be measured by increasing the testing load until the bone plate fails. This parameter has been measured in the literature [20, 23], and will provide further comparison between different bone plates and prior studies from the literature.

Four different testing trials, shown in Table 3.3, will be performed. The first trial will establish a baseline by testing a plate with standard geometry, similar to that in Figure 1-6. The second trial will evaluate the performance of the new bone plate in

its undeformed state. The third trial will evaluate plates that have been deformed by Dr. Seldin such as they would be during surgery. The plates for trials 1–3 will be fabricated by cutting 304 stainless steel on a waterjet. The same material will be used so that the results can be compared against each other. Finally, a fourth trial will be conducted using currently available bone plates. Results from this trial can be qualitatively compared to those from trials 1–3. Furthermore, the findings from trial 4 can be used to relate the work of this protocol to other studies found in the literature.

Table 3.4: List of Testing Trials

Trial	Bone Plate Type	Deformed Y/N	Material
1	Standard geometry	N	304 SS
2	New bone plate	N	304 SS
3	New bone plate	Y	404 SS
4	Currently available	N	Titanium

Chapter 4

Conclusions & Future Work

Malocclusion is a painful condition that can result from complications during mandibular fracture repair. A new bone plate design with a deformable region has been introduced with the intent of providing surgeons with a tool to help reduce the risk of malocclusion by enabling adjustment of fracture alignment after plate fixation.

A surgeon would use the new bone plate by applying a load to the deformable center section until the desired shape is achieved or observed alignment at the fracture site is improved. This load was predicted using beam theory models and numerical simulations. A testing jig was built to evaluate the deformation of the bone plate during loading. It was determined that a load between 350 N and 800 N is necessary to achieve deformation in the central section of the bone plate. This was most accurately predicted using a fixed-fixed beam model and a numerical simulation, each with a concentrated center load.

Performance of the bone plate was assessed through the design of an *in vitro* testing apparatus that simulates mandibular fixation and loading conditions. Two concepts were developed; one uses a synthetic mandible substrate to affix the bone plate in a configuration such that the performance of the plate is decoupled from that of the testing apparatus. The second concept, based off of ASTM and ISO standards, applies three-point bending to the bone plate while constrained in a mandibular configuration. These testing apparatuses differ from others found in the literature because they allow for consistent & repeatable testing for a variety of bone plate geometries, while

maintaining mandibular orientation. The goal of these testing methods is not to predict *in vivo* performance, but rather to provide a platform to reliably compare different bone plate performances against each other.

Future work will include further design iterations and fabrication of the testing apparatuses described in Section 3.2.3. Further numerical simulations can be created to predict bone plate performances in these apparatuses, and also to better predict the deformation of the center section. The beam models can be developed to include large deformation assumptions in order to more accurately predict the forces needed to deform the bone plate. Once the testing apparatuses are built, bone plates of various deformed geometries will be tested in conjunction with Alex Slocum, Jr. and Dr. Ed Seldin.

Appendix A

Beam Theory Matlab Script

```
%% Written by: Thomas Cervantes
%% Last modified: 5/10/11

function [] = BeamModels()
%% Calculates force needed to acheive specified yield stress
%% Also calculates displacement
%% Models used:
%% Fixed-Fixed, Concentrated center load
%% Fixed-Fixed, Distrbuted load
%% Cantilever, Distributed load
%% Cantilever, Concentrated load

clear all
clc

%% Define geometry of the beam
t = 0.00201;    %% thickness (m)
w = 0.00203;    %% width (m)
L = 0.004699;  %% length (m)

%%Calculate 2nd area moment of inertia
I = (t*w^(3))/12; %m^4

%% Define material properties of beam
E = 190000000000; % Modulus of Elasticity for AISI 304
YieldStrength = 206807000; % Yield Strength for AISI 304
```

```

%% Initialize Parameters
Force1 = 0;
Stress1 = 0;
Disp1 = 0;

Force2 = 0;
Stress2 = 0;
Disp2 = 0;

Force3 = 0;
Stress3 = 0;
Disp3 = 0;

Force4 = 0;
Stress4 = 0;
Disp4 = 0;

%% Define step size for force increment
dF = 1;

%%%%%%%%%%%%%%%%%%%%%%%%%%%%%%%%%%%%%%%%%%%%%%%%%%%%%%%%%%%%%%%%%%%%%%%%
% Scenario 1: Fixed-Fixed + Cantilever Beam; Concentrated Point Load %
%%%%%%%%%%%%%%%%%%%%%%%%%%%%%%%%%%%%%%%%%%%%%%%%%%%%%%%%%%%%%%%%%%%%%%%%
while Stress1 < YieldStrength

    P = Force1(end) + dF;
    Force1 = [Force1; P];

    %%Calculations for Element 1: Fixed-Fixed Beam with Concentrated Load at Center
    R1 = P/2; % Reaction force at fixed end
    M1_max = (P*L)/8; %Maximum moment at fixed ends
    M1_cmax = (P*L)/8; %Maximum moment at center
    d1_max = (P*L^3)/(192*E*I); %Maximum displacement
    sigma1_cmax = (M1_cmax*(w/2))/I; %Maximum bending stress at center in Element 1

    %%Calculations for Element 2A: Cantilever Beam with Concentrated Tip Load
    P2 = R1*sqrt(2)/2; %Bending force on Element 2 from reaction force
    d2A_max = (P2*L^3)/(3*E*I); %Maximum displacement

    %%Calculations for Element 2B: Cantilever Beam with End Moment
    M2B_max = M1_max; %Maximum moment (constant across length)
    d2B_max = (M2B_max*L^2)/(2*E*I); %Maximum displacement

    %%Final Calculations (stress, dtot)
    Disp1 = [Disp1; d1_max + (sqrt(2)/2)*(d2A_max + d2B_max)];

```

```

Stress1 = [Stress1; sigma1_cmax];
end

%Scenario 2: Fixed-Fixed + Cantilever Beam; Distributed Pressure Load
%%%%%%%%%%%%%%%%%%%%%%%%%%%%%%%%%%%%%%%%%%%%%%%%%%%%%%%%%%%%%%%%%%%%%%%%
while Stress2 < YieldStrength
    p = Force2(end) + dF;
    Force2 = [Force2; p];
    p = p/L;

    %Element 1: Fixed-Fixed Beam with Uniform Distributed Load w
    R1 = (p*L)/2; %Reaction force at fixed end
    M1_max = (p*L^2)/12; %Maximum moment at fixed ends
    M1_cmax = (p*L^2)/24; %Maximum moment at center
    d1_max = (p*L^4)/(384*E*I); %Maximum displacement
    sigma1_cmax = (M1_cmax*(w/2))/I; %Maximum bending stress at center

    %Element 2A: Cantilever Beam with Concentrated Tip Load
    P2 = R1*sqrt(2)/2; %Bending force on Element 2 from reaction force
    d2A_max = (P2*L^3)/(3*E*I); %Maximum displacement

    %Element 2B: Cantilever Beam with Applied Moment
    M2B_max = M1_max; %Maximum moment (constant across length)
    d2B_max = (M2B_max*L^2)/(2*E*I); %Maximum displacement

    %Final Calculations
    Disp2 = [Disp2; d1_max + (sqrt(2)/2)*(d2A_max + d2B_max)];
    Stress2 = [Stress2; sigma1_cmax];
end

%Scenario 3: Cantilever + Cantilever Beam; Distributed Pressure Load
%%%%%%%%%%%%%%%%%%%%%%%%%%%%%%%%%%%%%%%%%%%%%%%%%%%%%%%%%%%%%%%%%%%%%%%%
while Stress3 < YieldStrength
    P = Force3(end) + dF;
    Force3 = [Force3; P];
    p = P/L;

    %Element 1: Cantilever Beam with Uniform Distributed Load w
    R1 = p*L/2; % Reaction force at fixed end
    M1_max = ((p/2)*(L/2)^2)/2; % Maximum moment (at fixed end)
    d1_max = (p*(L/2)^4)/(8*E*I); %Maximum displacement
end

```

```

sigma_max = (M1_max*(w/2))/I; %Maximum bending stress at end
% Element 2A: Cantilever Beam with Concentrated Tip Load
P2 = R1*sqrt(2)/2; %Bending force on Element 2 from reaction force
d2A_max = (P2*L^3)/(3*E*I); %Maximum displacement
% Element 2B: Cantilever Beam with Applied Moment
M2B_max = M1_max; %Maximum moment (constant across length)
d2B_max = (M2B_max*L^2)/(2*E*I); %Maximum displacement
% Final Calculations
Disp3 = [Disp3; d1_max + (sqrt(2)/2)*(d2A_max + d2B_max)];
Stress3 = [Stress3; sigma_max];
end

% Scenario 4: Cantilever + Cantilever Beam; Concentrated Point Load
%%%%%%%%%%%%%%%%%%%%%%%%%%%%%%%%%%%%%%%%%%%%%%%%%%%%%%%%%%%%%%%%%%%%%%%%%%
while Stress4 > YieldStrength
P = Force4(end) + dF;
Force4 = [Force4; P];
% Calculations for Element 1: Cantilever Beam with Concentrated Load at Tip
R1 = P/2; % Reaction force at fixed end
M1_max = (P/2)*L; % Maximum moment (at fixed end)
d1_max = (P*L^3)/(3*E*I); %Maximum displacement
sigma_max = (M1_max*(w/2))/I; %Maximum bending stress at end
% Calculations for Element 2A: Cantilever Beam with Concentrated Tip Load
P2 = R1*sqrt(2)/2; %Bending force on Element 2 from reaction force
d2A_max = (P2*L^3)/(3*E*I); %Maximum displacement
% Calculations for Element 2B: Cantilever Beam with End Moment
M2B_max = M1_max; %Maximum moment (constant across length)
d2B_max = (M2B_max*L^2)/(2*E*I); %Maximum displacement
% Final Calculations (stress, dtot)
Disp4 = [Disp4; d1_max + (sqrt(2)/2)*(d2A_max + d2B_max)];
Stress4 = [Stress4; sigma_max];
end
disp('Cantilever model with concentrated load:');
disp(sprintf('Force to yielding = %d N',Force4(end)))
% Display Results
end

```

```
disp(sprintf('Displacement = %f mm\r',Disp4(end)*1000))
```

```
disp('Cantilever model with distributed load:')  
disp(sprintf('Force to yielding = %d N',Force3(end)))  
disp(sprintf('Displacement = %f mm\r',Disp3(end)*1000))
```

```
disp('Fixed-Fixed model with concentrated load:')  
disp(sprintf('Force to yielding = %d N',Force1(end)))  
disp(sprintf('Displacement = %f mm\r',Disp1(end)*1000))
```

```
disp('Fixed-Fixed model with distributed load:')  
disp(sprintf('Force to yielding = %d N',Force2(end)))  
disp(sprintf('Displacement = %f mm\r',Disp2(end)*1000))
```


Appendix B

Tolerance Calculations

B.1 Analysis for Concept 1 Shaft Misalignment

Misalignment at the bearing:

$$\sin(\theta) = \frac{d}{L_{bearing}}$$

Small angle approximation: $\sin(\theta) \approx \theta$

Misalignment at the center of the bone plate:

$$\sin(\theta) = \frac{2\Delta}{h_{plate}}$$

It is desired that $\frac{2\Delta}{h_{plate}} \leq 0.01$:

$$\sin\left(\frac{d}{L_{bearing}}\right) \leq 0.01$$

Given that $L_{bearing} = 1.987$ in, $d \leq 0.0196853675$ in .

B.2 Analysis for Concept 2 Gap Misalignment

Tilt in channel:

$$\sin(\theta) = \frac{2\delta}{h_{plate}}$$

Relationship between applied force and parasitic force:

$$\sin(\theta) = \frac{F_{parasitic}}{F_{applied}}$$

It is desired that $\frac{F_{parasitic}}{F_{applied}} \leq 0.01$

$$\sin\left(\frac{2\delta}{h_{plate}}\right) \leq 0.01$$

Given that the height of the plate, $h_{plate} = 0.5$ in, $\delta \leq 0.0025$ in.

Bibliography

- [1] Alper Alkan, Nukhet Celebi, Bora Ozden, Bureu Bas, and Samet Inal. Biomechanical comparison of different plating techniques in repair of mandibular angle fractures. *Oral Surgery Oral Medicine Oral Pathology Oral Radiology & Endodontics*, 104:752–756, 2007.
- [2] ASTM F382. *Standard Specification and Test Method for Metallic Bone Plates*. ASTM international, West conshohocken, PA, 2008.
- [3] Todd Bredbenner and Richard Haug. Substitutes for human cadaveric bone in maxillofacial rigid fixation research. *Oral Surgery Oral Medicine Oral Pathology Oral Radiology & Endodontics*, 90:574–80, 2000.
- [4] Thomas Chiodo, Vincent Ziccardi, Malvin Janal, and Christopher Sabitini. Failure Strength of 2.0 Locking Versus 2.0 Conventional Synthes Mandibular Plates: A Laboratory Model. *Journal of Oral & Maxillofacial Surgery*, 64:1475–79, 2006.
- [5] Byung-Ho Choi, Choong-Kook Yi, and Jae-Ha Yoo. Clinical Evaluation of 3 Types of Plate Osteosynthesis for Fixation of Condylar Neck Fractures. *Journal of Oral & Maxillofacial Surgery*, 59:734–737, 2001.
- [6] Ricardo Cienfuegos, Carl Cornelius, Edward Ellis, and George Kushner. Mandible—Special Considerations. <http://www.aofoundation.org>.
- [7] Matthew Craig, Cynthia Bir, David Viano, and Scott Tashman. Biomechanical response of the human mandible to impacts of the chin. *Journal of Biomechanics*, 41:2972–2980, 2008.
- [8] Dassault Systemes. Solidworks Simulation, 2010. Used with SolidWorks Student Edition 2010.
- [9] Arthur Dichard and Douglas Klotch. Testing Biomechanical Strength of Repairs for the Mandibular Angle Fracture. *Laryngoscope*, 104:201–208, February 1994.
- [10] Ellis E, Moos KF, and el Attar A. Ten years of mandibular fractures: An analysis of 2,137 cases. *Oral Surg Oral Med Oral Pathol*, 59:120–9, 1985.
- [11] FG Fedok, DW Van Kooten, LM DeJoseph, JD McGinn, B Sobota, RJ Levin, and CR Jacobs. Plating techniques and plate orientation in repair of mandibular angle fractures: an in vitro study. *Laryngoscope*, 108:1218–24, Aug 1998.
- [12] Jose Fernandez, M. Gallas, M. Burguera, and J.M. Viano. A three-dimensional numerical simulation of mandible fracture reduction with screwed miniplates. *Journal of Biomechanics*, 36:329–337, 2003.

- [13] Albert Fox and Robert Kellman. Mandibular Angle Fractures: Two-Miniplate Fixation and Complications. *Archives of Facial Plastic Surgery*, 5:464–69, 2003.
- [14] Kirk Fridrich, Gustavo Pena-Velasco, and Robert Olson. Changing Trends With Mandibular Fractures: A Review of 1,067 Cases. *Journal of Oral & Maxillofacial Surgery*, 50:586–89, 1992.
- [15] Andrew Gear, Elena Apasova, John Schmitz, and Waren Schubert. Treatment Modalities for Mandibular Angle Fractures. *Journal of Oral & Maxillofacial Surgery*, 63:655–63, 2005.
- [16] Kim Goldman. Ask An Oral & Maxillofacial Surgeon: Mandible Fractures. <http://www.calweb.com/goldman/index.html>.
- [17] R. C. Hibbeler. *Mechanics of Materials, 7th Edition*. Prentice Hall, 2008.
- [18] Instron. Static hydraulic testing system. Testing performed in April 2010.
- [19] ISO 9585. *Implants for surgery – Determination of bending strength and stiffness of bone plates*. International Organization for Standardization, Geneva, Switzerland, 1990.
- [20] Sonu Jain, Oliver Simmons, Michael Hanemann, Richard Baratta, Aldo Guerra, and Stephen Metzinger. Comparison of Tensile Strength of Resorbable Plating Systems Used in Monocortical Mandible Angle Osteotomy Repair. *Archives of Facial Plastic Surgery*, 8:390–395, 2006.
- [21] Chris Jarmey. *The Atlas of Musculo–Skeletal Anatomy*. North Atlantic Books, 2004.
- [22] Alex Slocum Jr. Personal interviews. 2011.
- [23] M. Karoglan, K. Shutz, H. Schieferstein, H. Horch, and A. Neff. Development of a static and dynamic simulator for osteosyntheses of the mandible. *Technology and Health Care*, 14:449–455, 2006.
- [24] Volkan Kovan. An assessment of impact strength of the mandible. *Journal of Biomechanics*, 41:3488–91, Dec 2008.
- [25] Scott Lovald, Tariq Khraishi, Jon Wagner, Bret Baack, James Kelly, and John Wood. Comparison of Plate-Screw Systems Used in Mandibular Fracture Reduction: Finite Element Analysis. *Journal of Biomechanical Engineering*, 128:654–662, October 2006.
- [26] Scott Lovald, Jon Wagner, and Bret Baack. Biomechanical Optimization of Bone Plates Used in Rigid Fixation of Mandibular Fractures. *Journal of Oral and Maxillofacial Surgery*, 67:973–985, 2009.
- [27] Mathworks. Matlab, R2010b.
- [28] Cory Resnick M.D. Personal interview. January 2011.
- [29] Gary Moore, Terry Olson, and Anthony Yonkers. A Retrospective Review of 100 Fractures in 56 Patients. *Nebraska Medical Journal*, pages 120–123, April 1985.
- [30] Pacific Research Laboratories. Sawbones, 2011. www.sawbones.com.

- [31] In-Phill Park, Seong-Joo Heo, Jai-Young Koak, and Seong-Kyun Kim. Post traumatic malocclusion and its prosthetic treatment. *J Adv Prosthodont*, 2:88–91, 2010.
- [32] Daniel Schwarz, Krigor Arman, Mehreen Kakwan, Ameen Jamali, and Steven Buchman. Analysis of the Biomechanical Properties of the Mandible after Unilateral Distraction Osteogenesis. *Plastic and Reconstructive Surgery*, 126:533–542, 2010.
- [33] Edward Seldin. Personal interviews. 2011.
- [34] Synthes. Synthescmf, 2010. www.synthes.com.
- [35] Hiroshi Watanabe, Momin Abdul, Tohru Kurabayashi, and Hideki Aoki. Mandible size and morphology determined with CT on a preminse of dental implant operation. *Surg Radiol Anat*, 32:343–49, 2010.
- [36] A. Ziebowicz and J. Marciniak. The use of miniplates in mandibular fractures– biomechanical analysis. *Journal of Materials Processing Technology*, 175:452–456, 2006.